PRAMANA
— journal of
physics

Vol. 74, No. 1
January 2010
pp. 75–82

Chaotic travelling rolls in Rayleigh–Bénard convection

SUPRIYO PAUL[1,*], KRISHNA KUMAR[2], MAHENDRA K VERMA[1], DANIELE CARATI[3], ARNAB K DE[4] and VINAYAK ESWARAN[4]
[1]Department of Physics, Indian Institute of Technology, Kanpur 208 016, India
[2]Department of Physics and Meteorology, Indian Institute of Technology, Kharagpur 721 302, India
[3]Physique Statistique et Plasmas, Université Libre de Bruxelles, B-1050 Bruxelles, Belgium
[4]Department of Mechanical Engineering, Indian Institute of Technology, Kanpur 208 016, India
*Corresponding author. E-mail: supriyo@iitk.ac.in

MS received 18 April 2009; revised 30 July 2009; accepted 11 August 2009

Abstract. In this paper we investigate two-dimensional (2D) Rayleigh–Bénard convection using direct numerical simulation in Boussinesq fluids with Prandtl number $P = 6.8$ confined between thermally conducting plates. We show through the simulation that in a small range of reduced Rayleigh number r ($770 < r < 890$) the 2D rolls move chaotically in a direction normal to the roll axis. The lateral shift of the rolls may lead to a global flow reversal of the convective motion. The chaotic travelling rolls are observed in simulations with free-slip as well as no-slip boundary conditions on the velocity field. We show that the travelling rolls and the flow reversal are due to an interplay between the real and imaginary parts of the critical modes.

Keywords. Convection; travelling rolls instability; direct numerical simulation.

PACS Nos 47.20.Bp, 47.20.-k

1. Introduction

The Rayleigh–Bénard convection (RBC) [1–3] is an extensively studied system for investigating a range of interesting phenomena like instabilities [4], pattern formation [5], chaos [6,7], spatio-temporal chaos and turbulence [8–10]. The convective flow is characterized by two non-dimensional numbers: the Rayleigh number R and the Prandtl number P. Two-dimensional (2D) stationary rolls [2] appear as primary instability in Boussinesq fluids confined between thermally conducting boundaries when the Rayleigh number R is raised just above a critical value R_c. The convective dynamics at higher values of R depends on Prandtl number. Interesting convective dynamics are observed when the Rayleigh number is increased beyond

R_c [4,11–14]. Busse [12] found travelling waves along the axis of the cylindrical rolls as secondary instability in low Prandtl number fluids that makes the convection three-dimensional (3D). Travelling waves are also found in rotating RBC in cylindrical geometry [15]. Another kind of travelling wave is known to occur in two-dimensional (2D) RBC in binary mixtures [16,17], where the straight rolls move in a direction perpendicular to the roll axis. Such behaviour is not reported in two-dimensional RBC in pure fluids, although many interesting features have been investigated (e.g., [18–20]).

In this paper we present results of two-dimensional numerical simulation of the RBC in a pure Boussinesq fluid of Prandtl number $P = 6.8$. A number of direct numerical simulations have been performed on 2D Rayleigh–Bénard convection [19–21]. Most of these work focus on evolution of energy, Nusselt number scaling, and flow patterns. Some of the numerical work also describe flow structures. However, detailed study of large-scale modes is still lacking, which is the main motivation for the present paper. We have used free-slip as well as no-slip boundary conditions on the velocity field at the horizontal plates. In the horizontal direction, we have assumed periodic boundary conditions on all the fields. We report our results as a function of reduced Rayleigh number $r = R/R_c$. For free-slip boundaries, at $r \approx 130$ we observe a transition from one oscillatory state with only real or imaginary values of critical modes W_{101} (corresponding to the vertical velocity component w) and θ_{101} (corresponding to temperature θ) to another oscillatory state where both the real and imaginary parts are nonzero. Later, when $770 < r < 890$ we find chaotic travelling waves in a direction normal to the roll-axis. The sudden lateral shift in the roll system leads to either jitters in the convective flow or flow reversal of the convective motion. The chaotic travelling waves are also observed in the direct numerical simulation (DNS) of the RBC with no-slip boundaries. We find links between the chaotic travelling waves or rolls and the flow reversal.

2. Hydrodynamic system

We consider 2D convection in an extended layer of Boussinesq fluid with thermal expansion coefficient α, kinematic viscosity ν, thermal diffusivity κ that is enclosed between two flat conducting plates separated by distance d and heated from below. The adverse temperature gradient is $\Delta T/d$, where ΔT is the temperature difference imposed across the bounding plates. The non-dimensional equations are

$$\frac{\partial \mathbf{v}}{\partial t} + (\mathbf{v}\cdot\nabla)\mathbf{v} = -\nabla\sigma + RP\theta\hat{\mathbf{z}} + P\nabla^2\mathbf{v}, \tag{1}$$

$$\frac{\partial \theta}{\partial t} + (\mathbf{v}\cdot\nabla)\theta = w + \nabla^2\theta. \tag{2}$$

Here the Rayleigh number $R = \alpha g(\Delta T)d^3/\nu\kappa$ is the ratio of the buoyancy and the dissipative forces, while the Prandtl number $P = \nu/\kappa$ is the ratio of thermal diffusive time $\tau_{\rm th} = d^2/\kappa$ and the viscous diffusive time $\tau_{\rm vis} = d^2/\nu$. The temperature perturbation θ due to the convective flow vanishes at thermally conducting

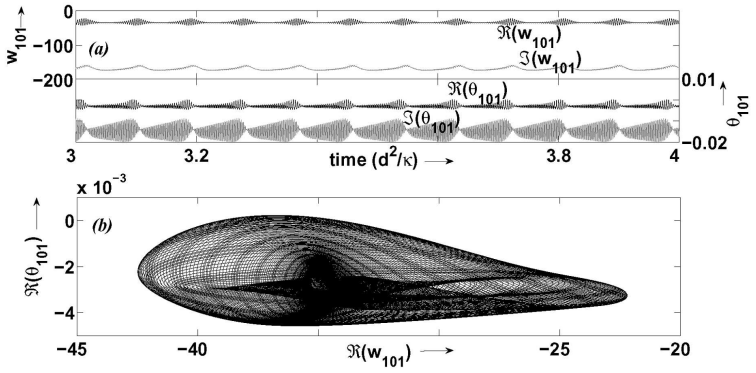

Figure 1. (**a**) Time series of $\Re(W_{101})$, $\Im(W_{101})$, $\Re(\theta_{101})$, $\Im(\theta_{101})$ at reduced Rayleigh number $r = 700$ and Prandtl number $P = 6.8$. The time series has two leading frequencies, and it shows quasiperiodic behaviour. (**b**) The projection of the phase space in $\Re(W_{101}) - \Re(\theta_{101})$ that elucidates the quasiperiodic behaviour of the system.

boundaries. The realistic no-slip boundary conditions imply that the velocity field $\mathbf{v} = (u, 0, w) = 0$ at the boundaries. The idealized free-slip boundaries imply $\partial_z u = w = 0$ at the flat plates. The value of R_c is $27\pi^4/4 \approx 657.5$ for free-slip boundaries and $R_c \approx 1707.8$ for no-slip boundaries.

We have carried out our simulations of the RBC in 2D using pseudo-spectral method [18] with stress-free boundaries. We use Fourier basis functions for representation along the x-direction, and sin or cos functions along the vertical z-direction. For example, the component of the velocity field in the z-direction is represented by

$$w(x, z, t) = \sum_{m,n} W_{m0n}(t) \mathrm{e}^{imk_c x} \sin(n\pi z), \tag{3}$$

where $k_c = \pi/\sqrt{2}$. Here the three subscripts of W denote the wavenumber indices of the Fourier modes along x-, y- and z-directions. In our simulation, the second subscript is always zero. The grid resolution used for the simulations with the free-slip boundaries is 256×256 with an aspect ratio of $2\sqrt{2} : 1$. The reduced Rayleigh number $r = R/R_c$ is varied from 1.01 to 10^3. We have employed fourth-order Runge–Kutta (RK4) scheme for time stepping with the time step varying from 1×10^{-4} to 1×10^{-6} in thermal diffusive time units. The code was validated using the results reported by Thual [18].

To solve no-slip convective flow, we employed two-step finite-difference procedure with the Adam–Bashforth–Crank–Nicolson scheme. The first step involves pressure calculation using Poisson's equation, and the second step deals with time-advancing using fourth-order central explicit scheme [22] with enhanced spectral resolution. We computed the no-slip flow for $r = 830$ and $P = 6.8$ and compared the results with that obtained with free-slip simulation.

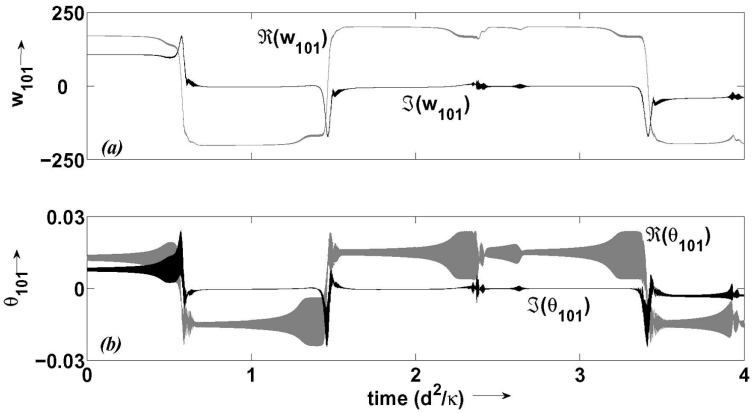

Figure 2. Time series of the real and imaginary parts of the critical velocity mode W_{101} (**a**) and the temperature mode θ_{101} (**b**) for $r = 830$. The origin on dimensionless time axis is suitably chosen after the steady state has been reached. The time series of the modes shows jitters (small fluctuations) and flips. The fluctuations in the temperature mode is stronger than that in the velocity mode.

3. Results

First we report the results of 2D simulation with free-slip boundary conditions. We observe long time behaviour of the critical 2D modes W_{101} and θ_{101}. We start our simulation with real Fourier modes. For reduced Rayleigh number $r \leq 80$, the system shows time-independent steady convection. For $80 < r < 130$, we observe simple oscillations in all the modes. Here all the Fourier modes remain real. Similar observations have been made previously by others [18–20]. As r is raised further, the critical Fourier modes (W_{101} and θ_{101}) become complex. For $130 < r < 145$, the imaginary parts of W_{101} and θ_{101} become nonzero and they oscillate around a zero mean, while the real parts oscillate around a nonzero mean.

For $145 < r < 770$ the imaginary parts of the complex modes also oscillate around a finite mean. This is an oscillatory instability, which makes the critical modes complex. The real and imaginary parts of a Fourier mode interact with each other through nonlinear interaction with higher-order modes. When the simulation is started with purely imaginary modes (except θ_{00n}, which is always real due to the reality condition), then the roles of real and imaginary parts of all complex modes get interchanged.

The oscillations of both real and imaginary parts become strongly anharmonic for $660 < r < 770$. This leads to temporally quasiperiodic flow. Figure 1a illustrates the real and the imaginary parts of the critical mode W_{101} and θ_{101}. These modes show two leading frequencies. The projection of phase space on $W_{101} - \theta_{101}$ shows quasiperiodic flow as seen in figure 1b. Similar behaviour has been observed in experiments on RBC by Swinney and Gollub [6].

The convection becomes chaotic for $770 < r < 890$. Figure 2 displays the real and the imaginary parts of the critical modes W_{101} and θ_{101} for $r = 830$. The

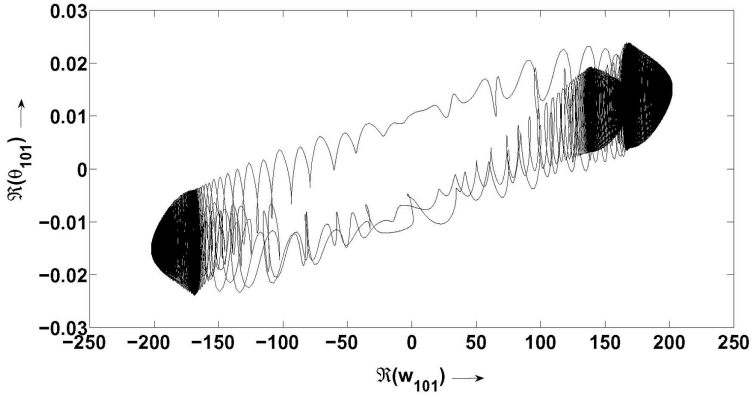

Figure 3. Projection of the phase space in the $\Re(W_{101})$–$\Re(\theta_{101})$ plane at $r = 830$. The figure illustrates the chaotic behaviour of the system.

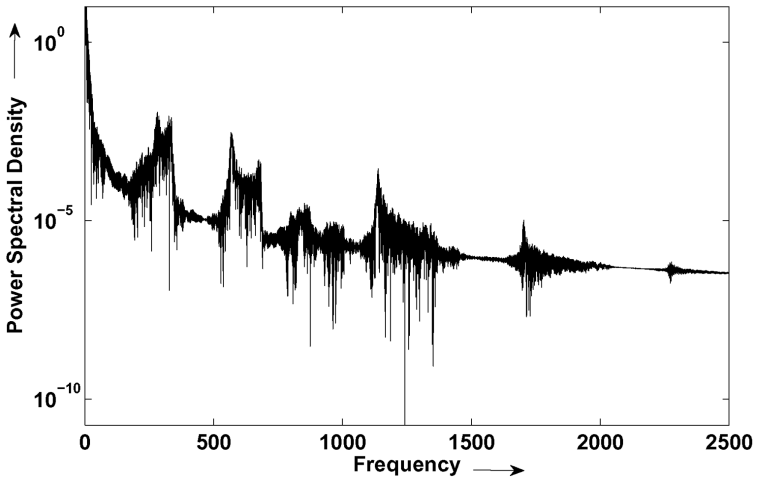

Figure 4. Power spectral density plot for the time signal of $\Re(W_{101})$ obtained from DNS of 2D RBC at $r = 830$ and $P = 6.8$.

projection of the phase space on $\Re(W_{101})$–$\Re(\theta_{101})$ plane is illustrated in figure 3 that indicates the chaotic nature of the system. The power spectral density (PSD) plot of the time signal of $\Re(W_{101})$ is shown in figure 4. The PSD shows a broad spectrum characteristic of a chaotic attractor.

In the chaotic regime, the real and imaginary parts of the critical modes interact strongly through nonlinear coupling with higher-order Fourier modes. As illustrated in figure 2, the Fourier modes show jitters (small fluctuations) as well as change in sign. The velocity mode W_{101} and temperature mode θ_{101} appear to be in approximate phase with each other. However, the fluctuations in the temperature mode near the jitter or the flip is stronger than the corresponding fluctuations in the velocity mode. The interval between two flips is of the order of one thermal diffusion time-scale, while the duration of the flips is much shorter.

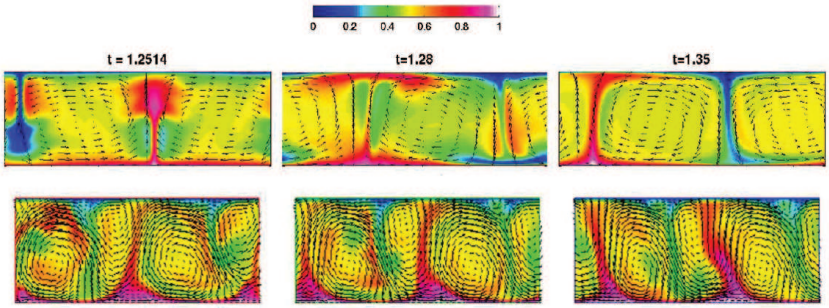

Figure 5. Travelling rolls in two-dimensional Rayleigh–Bénard convection at $r = 830$. The top panel of the figures is for the simulation with free-slip boundaries and the bottom panel is for the no-slip boundaries. The temperature field is represented in colour with blue being the coldest region. The arrows represent the velocity field. The three images at the top panel show the field configurations at three time. At $t = 1.2514$ the central region has hot fluid that shifts leftward subsequently. At $t = 1.35$ the whole roll pattern is shifted approximately by half a wavelength. Similar features are seen for no-slip convective flow, except that the flow pattern moves right.

The physical interpretation of the chaotic time series (figure 2) yields interesting insights into the travelling wave instability and flow reversal. We provide a simple argument to explain this. If the critical modes were the only modes in the system, then the vertical velocity in real space would be $\Re(W_{101}\exp(ik_c x)\sin(n\pi z))$. When W_{101} changes from a real value A to a complex value $A\exp(i\phi)$, it would lead to a shift of the roll pattern in horizontal distance by ϕ/k_c. This is the observed travelling wave instability near the bifurcation. Since the temporal change in the phase of the critical mode is chaotic, the movement of the rolls would also be irregular. During the flip of the critical Fourier modes, $\phi \approx \pi$, which corresponds to a horizontal shift of $\lambda/2$. Under this situation, the vertical velocity reverses its direction at a given location that leads to global flow reversal in the system. The simulated flow contains many modes apart from the critical modes, yet the large-scale ones play a dominant role. Hence, the bifurcation of the large-scale Fourier modes from real to complex plays a major role in initiating travelling wave instability and flow reversal.

We illustrate the above dynamics using figure 5 that contains two panels of images: the top ones are for the free-slip boundaries, while the bottom ones are for the no-slip boundaries. The two panels of figure 5 illustrate three snap-shots of the velocity and temperature at three different instances of time. The top panel (free-slip) illustrates the flow fields at $t = 1.2514$, $t = 1.28$ and $t = 1.35$ respectively for a different run. The temperature fields are shown in colour coding with blue being the coldest region, while the velocity fields are shown using arrows. At $t = 1.2514$, the hot fluid is rising near the centre. The roll pattern moves leftward as time advances. At time $t = 1.35$, a cold fluid parcel is falling down near the centre. Thus the top panel illustrates the travelling roll in RB convection under free-slip boundary condition. In the bottom panel, similar feature is observed for no-slip boundary condition, however, for a shorter time. Here the rolls have moved only

a smaller fraction of a wavelength. Note that the rolls are travelling perpendicular to the roll axis along the periodic direction in both the results, and the interval between two consecutive flow reversal is of the order of one diffusive time unit (refer to figure 2).

Figure 5 also depicts flow reversal phenomenon. If we place a probe near the centre of the system, we would observe the fluid to be hot and moving upward at initial time. At the end, the above-mentioned probe would measure colder fluid flowing downward. Thus a flow reversal due to travelling rolls is clearly illustrated.

We have created two movies to illustrate the travelling rolls and flow reversal by taking many frames between the reversal. These movies can be seen in our website [23,24]. The first movie [23] depicts the travelling rolls near a flow reversal regime. By the end of the movie (in approximately 0.1 thermal diffusive time unit), the roll has shifted approximately by half a wavelength. Similar features are observed in the second movie [24] that depicts the convective flow with no-slip boundaries; here the roll pattern moves to the right.

We have performed several three-dimensional (3D) simulations for Prandtl number 6.8, and a range of Rayleigh number in the chaotic and turbulent regime. We observe the above features of travelling rolls and flow reversal in 3D as well; these results will be reported in due course.

Reversal of large-scale flows has been observed in many experiments and numerical simulations [25–29]. Some of the experiments have been performed for large Rayleigh numbers (of the order of 10^9 to 10^{12}). The physics of the above phenomenon has been of great interest in the recent past. Our results are for two-dimensional RBC at moderately low Rayleigh numbers. Yet, the simple mechanism of travelling rolls in the periodic direction and its consequence to the phenomenon of flow reversal may be of interest in more complex situations. The large Rayleigh number regimes are under investigation.

4. Conclusion

To summarize, we observe succession of patterns in two-dimensional RBC under free-slip boundaries. Our focus has been on the chaotic travelling rolls observed in the range of $770 < r < 890$. We show that the generation of traveling rolls is due to the bifurcation of critical modes from real values to complex values. This kind of travelling roll is possible along the periodic direction that may be realized in practice along the azimuthal direction in a cylindrical container. It is interesting to note that several travelling roll states and flow reversals have been observed in cylindrical geometry. Also, the chaotic travelling rolls lead to flow reversal when the amplitude of the critical Fourier modes switches sign.

Acknowledgement

The author thank Stephan Fauve, Pankaj Mishra, K R Sreenivasan, J Niemela, and Bruno Eckhardt for discussions and various important suggestions. Part of the work was supported by the grant of Swarnajayanti Fellowship by the Department

of Science and Technology, India. Part of this work was done as the doctoral thesis work of SP.

References

[1] L Rayleigh, *Philos. Mag.* **32**, 529 (1916)
[2] S Chandrasekhar, *Hydrodynamic and hydromagnetic instability* (Oxford University Press, Oxford, 1961)
[3] F H Busse, *Rep. Prog. Phys.* **41**, 1929 (1978)
[4] E Bodenschatz, W Pesch and G Ahlers, *Annu. Rev. Fluid Mech.* **32**, 809 (2000)
[5] M C Cross and P C Hohenberg, *Rev. Mod. Phys.* **65**, 851 (1993)
[6] H L Swinney and J P Gollub, *Phys. Today* **31**, 41 (1978)
[7] S W Morris, E Bodenschatz, D S Cannell and G Ahlers, *Phys. Rev. Lett.* **71**, 2026 (1993)
[8] F H Busse, *Transition to turbulence in Rayleigh–Bénard convection (Hydrodynamic instabilities and the transition to turbulence)* (Springer, Berlin, 1981)
[9] P Manneville, *Instabilities, chaos, and turbulence* (Imperial College Press, London, 2004)
[10] G Ahlers, *Experiments with Rayleigh–Bénard convection (Dynamics of spatio-temporal structures – Henri Bénard centenary review)* (Springer, Berlin, 2005)
[11] G E Willis and J W Deardorff, *J. Fluid Mech.* **44**, 661 (1970)
[12] F H Busse, *J. Fluid Mech.* **52**, 97 (1972)
[13] R M Clever and F H Busse, *J. Fluid Mech.* **176**, 403 (1987)
[14] K Kumar, S Fauve and O Thual, *J. Phys. II (France)* **6**, 945 (1996)
[15] W Choi, D Prasad, R Camassa and R E Ecke, *Phys. Rev.* **E69**, 056301 (2004)
[16] R W Walden, P Kolodner, A Passner and C M Surko, *Phys. Rev. Lett.* **55**, 496 (1985)
[17] W Barten, M Lücke, W Hort and M Kamps, *Phys. Rev. Lett.* **63**, 376 (1989)
[18] O Thual, *J. Fluid Mech.* **240**, 229 (1992)
[19] D R Moore and N O Weiss, *J. Fluid Mech.* **58**, 289 (1973)
[20] J H Curry, J R Herring, J Loncaric and S A Orszag, *J. Fluid Mech.* **147**, 1 (1984)
[21] I Goldhirsch, R B Pelz and S A Orszag, *J. Fluid Mech.* **199**, 1 (1989)
[22] C K W Tam and J C Webb, *J. Comput. Phys.* **107**, 262 (1993)
[23] http://home.iitk.ac.in/˜mkv/Turbulence/Animations.html; the left movie depicts the convective flow for free-slip boundary condition
[24] http://home.iitk.ac.in/˜mkv/Turbulence/Animations.html; the right movie depicts the convective flow for no-slip boundary condition
[25] R Krishnamurti and L N Howard, *Proc. Natl. Acad. Sci. USA* **78**, 1981 (1981)
[26] J J Niemela, L Skrbek, K R Sreenivasan and R J Donnelly, *Nature (London)* **404**, 837 (2000)
[27] S Cioni, S Ciliberto and J Sommeria, *J. Fluid Mech.* **335**, 111 (1997)
[28] X-L Qiu and P Tong, *Phys. Rev.* **E64**, 036304 (2001)
[29] E Brown and G Ahlers, *J. Fluid Mech.* **98**, 137 (2006)